ISSN 1330–0016
CODEN FIZBE7

MAIN PECULIARITIES OF THE CASCADE γ-DECAY PROCESS OF THE ^{176}Lu COMPOUND NUCLEUS

VALERY A. KHITROV[a], ANATOLY M. SUKHOVOJ[a], JAROSLAV HONZÁTKO[b], IVO TOMANDL[b] and GEORGY GEORGIEV[c]

[a] *Frank Laboratory of Neutron Physics, Joint Institute for Nuclear Research, 141980 Dubna, Russia*

[b] *Nuclear Physics Institute, CZ-25068 Řež near Prague, Czech Republic*

[c] *Institute for Nuclear Research and Nuclear Energy, 1784 Sofia, Bulgaria*

Received 12 June 1997; revised manuscript received 26 November 1998
Accepted 29 March 1999

The two-step γ-cascades, following thermal neutron capture in ^{175}Lu and terminating at 14 low-lying ($E_{ex} < 600$ keV) levels or level doublets of the ^{176}Lu nucleus, have been studied using the sum-coincidence technique using two Ge-detectors. The parameter majority of these cascades was unambiguously placed in the decay scheme. The regularity in the energies of the most intense cascades has been revealed. The results are compared with previous data for a group of deformed and spherical nuclei and with predictions of different models.

PACS numbers: 25.40.LW, 27.70.+q, 27.60.+j UDC 539.172.4
PACS Keywords: ^{176}Lu states, thermal neutron capture in ^{175}Lu, two-step γ-cascades, sum-coincidence technique

1. Introduction

The search for the population and decay process of deformed nuclei above the excitation energy of 1 MeV for odd-odd and 2 MeV for even-even nuclei allows a detailed study of the dynamics of the intricate nuclear structure at its transition from the "order"

of practically single-component wave functions of the low-lying levels to the "chaos" of millions of components of the neutron resonance wave function.

Such a possibility has appeared since it was ascertained at the Laboratory of Neutron Physics in Dubna that the known method of amplitude summation of coinciding pulses from two Ge-detectors allows one to distinguish and study both the sufficiently intense cascades [1] and the total contribution of the low-intensity cascades [2] which proceed from the compound state to a given low-lying level of any nucleus in the energy region up to the neutron binding energy, B_n. From the group of such distributions obtained for a specific nucleus, one can easily [3] and reliably [4] construct the scheme of nuclear levels excited by the cascades with intensities higher than about 10^{-4} per decay. On the basis of these data, one can find the dependence of the total cascade intensities (summed in some energy bins) on the nuclear excitation energy. This can be done for both experimentally resolved and unresolved cascades.

In order to reveal the most general peculiarities of the cascade γ-decay process following the neutron resonance capture, it is important to study it for the largest possible set of nuclei.

2. Experiment

The experiment was performed at the LWR-15 research reactor at Řež using a facility installed at the thermal neutron beam from a neutron guide tube [5]. The target was 1 g sample of the ^{175}Lu isotope, enriched to 99.8%. The γγ-coincidences were registered by a system using a 20% HPGe detector and a 12% Ge(Li) detector. The data acquisition time was about 560 hours. A part of the summed amplitudes of coincident pulses is shown in Fig. 1. The coincidences corresponding to the full energy peaks in this spectrum were used to construct the intensity distributions of two-step cascades proceeding from the compound state to low-lying levels of ^{176}Lu.

The target provided approximately 80% of neutron captures in ^{175}Lu and 20% in the ^{176}Lu impurity isotope. In this situation, isotopic identification of peaks in the sum-coincidence spectrum was performed using the known data on the level schemes and on neutron binding energies B_n for ^{176}Lu and ^{177}Lu. The best correspondence between the energies of the cascades and positions of the corresponding peaks for both isotopes in the sum-coincidence spectrum was achieved when using B_n=6289.3 keV for ^{175}Lu and 7072.4 keV for ^{176}Lu. These B_n values and the energies of the final levels of cascades from the available compilations were used for normalization of the cascade transition energies in Table 1. If one uses the value B_n=6287.9 keV, then the energies of cascade transitions in Table 1 will be somewhat lower, and that requires to decrease B_n of ^{177}Lu to 7071.0 keV.

To reject annihilation quanta, the coincidence detection level was set at 520 keV. This detection threshold was used for the normalization of data listed in Table 1. The parameters of the cascades in which energy of one of the quanta is less than the detection threshold are also given in Table 1.

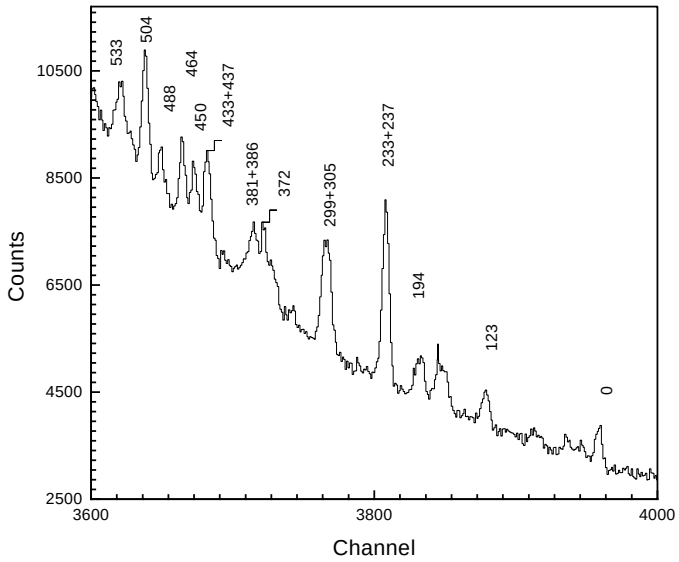

Fig. 1. Part of the sum-coincidence spectrum of ^{176}Lu*. Figures marking the peaks denote the energies (in* keV*) of the final cascade levels.*

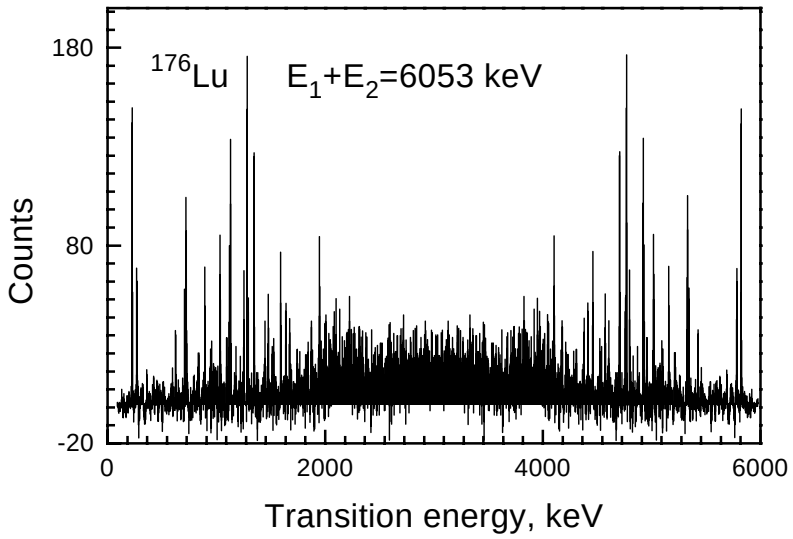

Fig. 2. The intensity distribution of two-step cascades with a total energy of 6053 keV*.*

In this way, one can detect all possible two-step cascades through any intermediate state lying 520 keV below the neutron binding energy and 520 keV above the excitation energy of the final level. An example of such a distribution is shown in Fig. 2. All of these distributions were built using the numerical method for improving the energy resolution [6]. As a result, the widths of the peaks change from 3.2 keV at the ends to 3.5 keV

at the centre of any spectrum. From the positions and areas of the resolved peaks, the transition energies and intensities of 350 cascades were derived. These data allowed the determination of energies of 230 levels (as a maximum). All these data are listed in Table 1. The area of each of spectrum was normalised to 100%. Due to the experimental limitations, Table 1 gives the lower estimates of the intensities for the cascades if the energy of one of the cascade transitions is less than 520 keV.

If the intermediate level of a cascade is depopulated by a pair of sufficiently intense secondary transitions, then the quanta ordering in the corresponding cascades was determined by means of the algorithm of Ref. 3. The intermediate energies E_m of these levels, that were determined using the maximum likelihood method, are also given in Table 1.

TABLE 1. A list of energies, E_1 and E_2, of measured cascade transitions and their relative intensities, $i_{\gamma\gamma} \pm \Delta i_{\gamma\gamma}$, in percent of the total intensity of the two-step cascades which have the same total energy. $E_m \pm \Delta E_m$ is the intermediate level energy. E_f is the energy of the final levels of the cascades [7].

E_1 (keV)	E_2 (keV)	$i_{\gamma\gamma}(\Delta i_{\gamma\gamma})$	$E_m(\Delta E_m)$(keV)
E_1+E_2 =6289.3 keV; E_f = 0 keV			
5402.5	886.9(6)	0.59(18)	886.7(5)
5365.7	923.7(9)	1.73(99)	922.4(9)
5454.7	834.6(1)	2.58(24)	(834.6)
5386.7	902.6(5)	0.71(18)	(902.6)
5368.7	920.6(9)	3.12(47)	(920.6)
5317.2	972.1(6)	0.56(18)	(972.1)
5257.1	1032.2(4)	1.21(24)	(1032.2)
4679.6	1609.7(6)	0.91(28)	(1609.7)
4570.1	1719.2(7)	0.77(27)	(1719.2)
4525.3	1764.0(6)	0.89(27)	(1764.0)
E_1+E_2 =6166.3 keV; E_f=122.9 keV			
5598.8	567.6(5)	0.47(13)	690.0(5)
5458.7	707.7(3)	0.53(10)	830.4(5)
5403.3	763.1(6)	0.46(15)	886.7(5)
5342.9	823.5(6)	0.73(26)	946.0(4)
5328.9	837.6(4)	1.07(27)	961.0(5)
5259.3	907.1(4)	1.27(26)	1029.7(5)
5063.3	1103.1(5)	1.05(28)	1226.6(4)
5057.8	1108.6(6)	0.84(28)	1231.0(9)
4962.8	1203.7(4)	1.34(29)	1328.5(12)
4922.7	1243.7(1)	4.69(51)	1365.5(8)
4770.9	1395.5(2)	3.36(51)	1519.2(12)
4681.6	1484.8(4)	1.53(35)	1607.6(3)
4607.6	1558.8(4)	1.65(35)	1681.7(7)

Table 1. (continued)

E_1, keV	E_2, keV	$i_{\gamma\gamma}(\Delta i_{\gamma\gamma})$	$E_m(\Delta E_m)$, keV
4016.9	2149.6(4)	1.82(46)	2272.2(4)
3897.1	2269.3(5)	1.51(46)	2392.3(4)
3888.5	2278.0(3)	1.74(39)	2401.1(3)
5984.0	182.5(1)	2.93(27)	(305.3)
5900.7	265.8(5)	0.65(18)	(388.6)
5855.7	310.7(2)	1.93(23)	(433.6)
5648.3	516.8(4)	0.60(15)	(641.0)
5603.6	561.4(4)	0.82(17)	(685.7)
5435.7	729.2(6)	0.36(12)	(853.6)
5226.9	939.6(2)	1.96(32)	(1062.4)
4987.9	1178.0(7)	0.76(27)	(1301.4)
4960.0	1209.6(4)	1.04(24)	(1329.3)
4932.8	1233.7(2)	2.71(39)	(1356.5)
4781.8	1384.3(6)	0.96(32)	(1507.5)
4657.8	1508.6(7)	0.89(32)	(1631.5)
4344.6	1821.5(5)	1.51(44)	(1944.7)
4268.4	1898.0(4)	2.00(46)	(2020.9)
3987.1	2179.0(3)	2.38(52)	(2302.2)
$E_1 + E_2$ =6094.7 keV; E_f=194.4 keV			
5827.5	267.1(6)	0.41(14)	462.0(4)
5729.2	365.5(1)	2.50(23)	560.4(3)
5259.6	835.0(2)	1.24(18)	1029.7(5)
5123.4	971.3(3)	1.01(20)	1165.6(3)
5107.9	986.8(3)	1.22(21)	1181.5(10)
5096.0	998.7(5)	0.70(18)	1193.7(7)
5062.5	1032.2(4)	0.76(19)	1226.6(4)
4770.8	1323.9(4)	0.94(22)	1519.2(12)
4608.6	1486.1(5)	0.76(22)	1681.7(7)
4512.4	1582.3(6)	0.72(22)	1776.9(4)
4458.0	1636.7(5)	0.79(22)	1831.5(4)
5784.1	310.7(2)	1.20(17)	(505.2)
5573.2	521.6(2)	1.17(18)	(716.1)
5368.2	726.6(5)	0.59(16)	(921.1)
5349.9	744.9(4)	0.87(20)	(939.4)
5232.8	862.0(1)	2.58(26)	(1056.5)
5196.9	897.9(5)	0.57(16)	(1092.4)
5080.3	1014.5(3)	1.08(19)	(1209.0)
5055.1	1039.7(3)	0.94(19)	(1234.2)
5028.5	1066.3(2)	1.34(20)	(1260.8)
4908.2	1186.6(7)	0.63(22)	(1381.1)
4871.1	1223.7(3)	1.42(25)	(1418.2)
4534.5	1560.3(6)	0.65(22)	(1754.8)
4421.8	1673.0(5)	0.92(24)	(1867.5)

Table 1. (continued)

E_1, keV	E_2, keV	$i_{\gamma\gamma}(\Delta i_{\gamma\gamma})$	$E_m(\Delta E_m)$, keV
E_1+E_2 =6055.9 keV; E_f=233.1+235.8 keV			
5827.2	228.6(1)	2.13(15)	462.0(4)
5470.6	585.3(4)	0.15(4)	818.9(3)
5458.9	596.9(3)	0.23(4)	830.4(5)
5429.9	626.0(1)	0.55(5)	859.6(4)
5333.1	722.7(1)	1.48(13)	957.2(12)
5328.6	727.2(3)	0.55(8)	961.0(5)
5159.9	895.9(2)	0.80(11)	1129.8(4)
5108.5	947.3(3)	0.35(7)	1181.5(10)
5096.7	959.1(3)	0.35(8)	1193.7(7)
5062.6	993.3(5)	0.24(7)	1226.6(4)
5057.1	998.7(6)	0.23(7)	1231.0(9)
5020.9	1034.9(1)	1.23(13)	1269.1(6)
5016.3	1039.5(5)	0.31(8)	1273.1(4)
4959.7	1096.1(3)	0.50(9)	1328.5(12)
4935.0	1120.8(1)	0.94(11)	1354.2(8)
4924.6	1131.2(1)	1.71(14)	1365.5(8)
4834.6	1221.2(5)	0.26(7)	1456.6(11)
4772.1	1283.7(1)	2.65(17)	1516.9(4)
4761.4	1294.5(2)	0.80(10)	1528.0(3)
4708.4	1347.4(1)	1.97(15)	1582.3(9)
4608.2	1447.6(3)	0.42(8)	1681.7(7)
4577.1	1478.7(2)	0.74(10)	1712.7(5)
4170.3	1885.6(6)	0.27(9)	2119.1(4)
3971.1	2084.8(3)	0.59(12)	2318.2(4)
5785.8	270.1(1)	0.99(10)	(503.5)
5694.8	361.1(4)	0.25(5)	(594.5)
5632.0	423.9(5)	0.19(5)	(657.3)
5345.6	710.3(1)	0.80(9)	(943.7)
5215.5	840.4(3)	0.36(7)	(1073.8)
4888.1	1167.8(6)	0.21(7)	(1401.2)
4875.0	1180.9(4)	0.32(7)	(1414.3)
4801.1	1254.8(2)	0.85(11)	(1488.2)
4614.3	1441.6(5)	0.25(6)	(1675.0)
4541.3	1514.6(3)	0.39(7)	(1748.0)
4526.9	1529.0(3)	0.44(8)	(1762.4)
4462.9	1593.0(1)	1.03(11)	(1826.4)
4416.3	1639.6(2)	0.73(10)	(1873.0)
4381.4	1674.5(2)	0.62(9)	(1907.9)
4311.5	1744.4(4)	0.40(8)	(1977.8)
4287.6	1768.3(6)	0.22(7)	(2001.7)
4234.9	1821.0(4)	0.29(7)	(2054.4)
4225.4	1830.5(5)	0.23(7)	(2063.9)

Table 1. (continued)

E_1, keV	E_2, keV	$i_{\gamma\gamma}(\Delta i_{\gamma\gamma})$	$E_m(\Delta E_m)$, keV
4217.4	1838.6(5)	0.26(7)	(2071.9)
4211.9	1844.0(5)	0.28(8)	(2077.4)
4180.8	1875.1(3)	0.66(12)	(2108.5)
4106.4	1949.5(2)	1.15(16)	(2182.9)
4100.1	1955.8(4)	0.39(10)	(2189.2)
4078.7	1977.2(6)	0.28(9)	(2210.6)
4048.6	2007.4(3)	0.65(12)	(2240.7)
4005.4	2050.5(5)	0.41(11)	(2283.9)
3981.3	2074.6(4)	0.42(11)	(2308.0)
3953.7	2102.2(3)	0.56(13)	(2335.6)
3856.4	2199.5(5)	0.41(12)	(2432.9)
3852.1	2203.8(6)	0.39(12)	(2437.2)
3830.4	2225.6(4)	0.63(13)	(2458.9)
E_1+E_2 =5987.9 keV; E_f=299.4+305.3 keV			
5728.5	259.3(2)	0.71(9)	560.4(3)
5599.4	388.5(5)	0.26(7)	690.0(5)
5563.9	423.9(1)	1.06(10)	725.1(3)
5333.8	654.1(5)	0.26(8)	957.2(12)
5327.8	660.1(3)	0.63(11)	961.0(5)
5124.2	863.7(5)	0.39(11)	1165.6(3)
5106.5	881.3(2)	0.83(13)	1181.5(10)
5016.0	971.8(3)	0.58(11)	1273.1(4)
4960.3	1027.6(4)	0.46(10)	1328.5(12)
4923.6	1064.2(2)	1.18(15)	1365.5(8)
4769.4	1218.5(4)	0.46(11)	1519.2(12)
4611.1	1376.8(2)	1.13(16)	1677.0(7)
4604.3	1383.6(4)	0.59(12)	1684.8(3)
4428.2	1559.7(6)	0.38(12)	1861.3(5)
4358.4	1629.5(7)	0.36(12)	1930.7(4)
4170.1	1817.7(4)	0.50(12)	2119.1(4)
4054.6	1933.3(5)	0.55(15)	2234.7(4)
5754.3	233.6(2)	0.52(9)	(535.0)
5652.3	335.6(2)	0.52(8)	(637.0)
5569.1	418.8(6)	0.23(8)	(720.2)
5408.5	579.4(1)	3.72(22)	(880.8)
5224.5	763.4(4)	0.33(8)	(1064.8)
5060.7	927.2(4)	0.48(11)	(1228.6)
4940.3	1047.6(5)	0.38(10)	(1349.0)
4873.6	1114.3(4)	0.42(10)	(1415.7)
4847.8	1140.1(5)	0.38(10)	(1441.5)
4775.5	1212.4(5)	0.44(11)	(1513.8)
4732.6	1255.3(5)	0.38(11)	(1556.7)
4474.3	1513.6(6)	0.34(11)	(1815.0)

Table 1. (continued)

E_1, keV	E_2, keV	$i_{\gamma\gamma}(\Delta i_{\gamma\gamma})$	$E_m(\Delta E_m)$, keV
4414.3	1573.6(2)	1.17(17)	(1875.0)
4377.8	1610.1(6)	0.35(11)	(1911.5)
4313.4	1674.5(6)	0.36(11)	(1975.9)
4308.1	1679.8(4)	0.51(12)	(1981.2)
4213.7	1774.2(6)	0.34(11)	(2075.6)
4160.5	1827.4(6)	0.37(11)	(2128.8)
E_1+E_2 =5916.6 keV; E_f=372.5 keV			
5330.2	586.3(5)	0.44(12)	957.2(12)
5095.0	821.6(3)	0.75(16)	1193.7(7)
5020.2	896.4(2)	1.52(19)	1269.1(6)
5014.3	902.2(3)	0.83(16)	1274.8(3)
4983.7	932.8(7)	0.42(15)	1306.6(9)
4979.1	937.5(7)	0.42(15)	1309.0(9)
4831.8	1084.8(1)	2.59(28)	1456.6(11)
4772.8	1143.8(5)	0.58(15)	1516.9(4)
4681.8	1234.8(6)	0.45(16)	1607.6(3)
4612.5	1304.1(3)	1.07(24)	1677.0(7)
4607.9	1308.7(5)	0.77(21)	1681.7(7)
4575.8	1340.8(5)	0.68(19)	1712.7(5)
4373.5	1543.1(4)	0.81(21)	1915.5(4)
5335.8	580.9(4)	0.48(12)	(953.5)
5077.3	839.4(6)	0.42(14)	(1212.0)
5000.6	916.1(5)	0.56(14)	(1288.7)
4663.5	1253.2(3)	0.94(18)	(1625.8)
4625.6	1291.1(6)	0.62(19)	(1663.7)
4430.0	1486.7(5)	0.73(20)	(1859.3)
E_1+E_2 =5902.6 keV; E_f=381.4+386.6 keV			
5328.7	573.9(4)	0.64(12)	961.0(5)
5258.9	643.7(1)	1.89(22)	1029.7(5)
5018.1	884.5(4)	0.59(15)	1271.4(4)
4981.9	920.7(5)	0.57(16)	1306.6(9)
4962.4	940.2(5)	0.52(15)	1328.5(12)
4928.3	974.3(5)	0.55(15)	1361.5(4)
4768.2	1134.3(3)	1.15(21)	1519.2(12)
4707.3	1195.2(4)	0.75(18)	1582.3(9)
4681.8	1220.8(2)	2.10(27)	1607.6(3)
4374.2	1528.4(5)	0.59(17)	1915.5(4)
4368.7	1533.9(7)	0.50(17)	1920.8(5)
4165.5	1737.0(6)	0.50(17)	2123.3(4)
5324.6	578.0(3)	0.78(13)	(964.7)
4812.8	1089.8(5)	0.55(16)	(1476.5)
4717.6	1185.0(4)	0.89(19)	(1571.7)
4659.1	1243.4(6)	0.56(14)	(1630.2)

Table 1. (continued)

E_1, keV	E_2, keV	$i_{\gamma\gamma}(\Delta i_{\gamma\gamma})$	$E_m(\Delta E_m)$, keV
4597.9	1304.7(4)	0.78(18)	(1691.4)
4549.8	1352.8(7)	0.56(18)	(1739.5)
4267.6	1635.0(5)	0.66(17)	(2021.7)
4156.8	1745.8(5)	0.60(17)	(2132.5)
E_1+E_2 =5851.9 keV; E_f=433.0+437.3 keV			
5331.3	520.5(3)	0.92(14)	957.2(12)
5327.7	524.2(1)	2.59(20)	961.0(5)
5106.5	745.3(5)	0.41(12)	1181.5(10)
4980.2	871.7(4)	0.68(17)	1309.0(9)
4924.5	927.4(2)	1.52(21)	1365.5(8)
4831.5	1020.4(4)	0.77(16)	1456.6(11)
4768.4	1083.4(3)	0.83(16)	1519.2(12)
4706.6	1145.3(2)	1.66(25)	1582.3(9)
4612.8	1239.0(2)	2.75(35)	1677.0(7)
4608.5	1243.3(7)	0.83(27)	1681.7(7)
4604.8	1247.1(3)	1.61(31)	1684.8(3)
4427.6	1424.2(7)	0.44(15)	1861.3(5)
4368.5	1483.4(6)	0.52(15)	1920.8(5)
5626.9	225.0(1)	1.84(18)	(662.4)
5256.1	595.8(4)	0.57(12)	(1033.2)
5184.6	667.3(3)	0.78(12)	(1104.7)
5156.5	695.4(2)	1.00(13)	(1132.8)
5012.9	839.0(5)	0.56(16)	(1276.4)
4930.2	921.7(6)	0.45(15)	(1359.1)
4759.7	1092.2(1)	2.29(25)	(1529.6)
4725.2	1126.7(4)	0.82(21)	(1564.1)
4678.5	1173.4(3)	1.24(22)	(1610.8)
4544.7	1307.2(7)	0.44(15)	(1744.6)
4521.3	1330.6(6)	0.48(15)	(1768.0)
4470.1	1381.8(5)	0.54(15)	(1819.2)
4342.1	1509.8(4)	0.64(15)	(1947.2)
4336.1	1515.8(6)	0.51(15)	(1953.2)
4128.7	1723.2(7)	0.62(20)	(2160.6)
4096.0	1755.9(6)	0.60(18)	(2193.3)
4058.8	1793.1(7)	0.55(19)	(2230.5)
4053.7	1798.2(4)	0.93(21)	(2235.6)
E_1+E_2 =5839.0 keV; E_f=450.1 keV			
5470.3	368.7(1)	1.42(15)	818.9(3)
5259.9	579.0(4)	0.77(19)	1029.7(5)
5094.5	744.5(5)	0.68(18)	1193.7(7)
5017.8	821.2(5)	0.97(25)	1271.4(4)
4934.2	904.7(6)	0.82(25)	1354.2(8)

Table 1. (continued)

E_1, keV	E_2, keV	$i_{\gamma\gamma}(\Delta i_{\gamma\gamma})$	$E_m(\Delta E_m)$, keV
4924.1	914.8(5)	0.84(25)	1365.5(8)
4833.8	1005.2(5)	0.85(25)	1456.6(11)
4771.0	1067.9(1)	3.58(39)	1519.2(12)
4607.2	1231.8(4)	1.03(22)	1681.7(7)
4599.1	1239.9(6)	0.64(22)	1690.1(5)
4358.7	1480.3(3)	1.70(29)	1930.7(4)
4029.4	1809.5(5)	1.10(29)	2258.8(8)
4017.4	1821.5(6)	0.92(28)	2272.2(4)
3897.0	1942.0(6)	1.00(33)	2392.3(4)
3888.2	1950.8(4)	1.61(34)	2401.1(3)
5111.4	727.6(6)	0.52(18)	(1177.9)
4800.1	1038.9(4)	1.10(25)	(1489.2)
3920.9	1918.1(5)	1.09(32)	(2368.4)
3824.8	2014.2(6)	1.13(37)	(2464.5)
3781.6	2057.4(6)	0.89(32)	(2507.7)
E_1+E_2 =5825.4 keV; E_f=463.8 keV			
5367.2	458.2(3)	1.30(27)	922.4(9)
5260.5	564.9(4)	0.91(21)	1029.7(5)
4927.5	897.9(4)	1.11(26)	1361.5(4)
4706.7	1118.7(6)	0.79(25)	1582.3(9)
4606.4	1219.0(4)	1.22(25)	1681.7(7)
4054.7	1770.7(5)	0.98(27)	2234.7(4)
3888.1	1937.3(3)	1.66(34)	2401.1(3)
5406.5	418.9(2)	2.26(32)	(882.8)
5246.8	578.6(2)	2.34(28)	(1042.5)
4985.9	839.5(2)	2.86(38)	(1303.4)
4763.9	1061.5(5)	1.02(28)	(1525.4)
4632.1	1193.3(6)	0.79(25)	(1657.2)
4538.5	1286.9(6)	0.76(25)	(1750.8)
4510.7	1314.7(6)	0.73(25)	(1778.6)
4316.8	1508.6(5)	0.86(23)	(1972.5)
3965.0	1860.4(4)	1.27(28)	(2324.3)
E_1+E_2 =5801.5 keV; E_f=487.6 keV			
5343.5	458.0(1)	8.44(75)	946.0(4)
4961.0	840.5(5)	1.87(54)	1328.5(12)
4936.3	865.2(6)	1.65(53)	1354.2(8)
4923.8	877.7(5)	1.88(53)	1365.5(8)
4831.7	969.8(5)	1.94(53)	1456.6(11)
4705.4	1096.1(6)	1.62(54)	1582.3(9)
4837.0	964.6(7)	1.53(53)	(1452.3)
E_1+E_2 =5784.3 keV; E_f=504.9 keV			
5445.6	338.7(2)	1.60(20)	843.8(4)

Table 1. (continued)

E_1, keV	E_2, keV	$i_{\gamma\gamma}(\Delta i_{\gamma\gamma})$	$E_m(\Delta E_m)$, keV
5159.1	625.1(4)	0.51(12)	1129.8(4)
5123.7	660.6(6)	0.37(12)	1165.6(3)
5109.1	675.2(4)	0.49(12)	1181.5(10)
5095.3	689.0(1)	3.04(21)	1193.7(7)
4922.6	861.7(5)	0.50(14)	1365.5(8)
4770.3	1014.0(5)	0.64(17)	1519.2(12)
4707.0	1077.3(6)	0.51(17)	1582.3(9)
4607.7	1176.6(2)	1.67(23)	1681.7(7)
4599.2	1185.1(6)	0.54(17)	1690.1(5)
4539.5	1244.8(6)	0.48(17)	1749.8(4)
3971.1	1813.1(5)	0.65(19)	2318.2(4)
5566.9	217.4(5)	0.47(14)	(722.4)
5416.5	367.8(2)	1.43(20)	(872.8)
5187.7	596.5(4)	0.56(12)	(1101.6)
4946.1	838.2(1)	2.63(26)	(1343.2)
4886.5	897.8(5)	0.50(14)	(1402.8)
4189.5	1594.8(5)	0.64(16)	(2099.8)
4174.2	1610.1(4)	0.68(16)	(2115.1)
4145.7	1638.6(4)	0.70(16)	(2143.6)
4110.2	1674.1(6)	0.52(16)	(2179.1)
4104.4	1679.9(5)	0.55(16)	(2184.9)
3959.0	1825.3(6)	0.61(18)	(2330.3)
3790.7	1993.6(4)	0.76(19)	(2498.6)
3777.5	2006.8(5)	0.72(19)	(2511.8)
3764.9	2019.4(4)	0.86(20)	(2524.4)
$E_1 + E_2$ =5756.1 keV; E_f=533.1 keV			
5564.4	191.6(2)	0.94(14)	725.1(3)
5446.0	310.1(1)	2.58(22)	843.8(4)
5331.9	424.2(1)	1.76(18)	957.2(12)
5096.1	659.9(5)	0.43(12)	1193.7(7)
5059.3	696.7(5)	0.45(12)	1231.0(9)
5019.5	736.6(4)	0.62(13)	1269.1(6)
5014.7	741.4(4)	0.57(12)	1274.8(3)
4981.5	774.5(3)	0.59(12)	1309.0(9)
4925.1	831.0(7)	0.56(19)	1365.5(8)
4833.2	922.9(4)	0.76(16)	1456.6(11)
4612.8	1143.2(3)	1.10(19)	1677.0(7)
4604.5	1151.6(5)	0.68(18)	1684.8(3)
4166.2	1589.9(4)	0.66(15)	2123.3(4)
4031.4	1724.7(5)	0.61(16)	2258.8(8)
5089.6	666.5(6)	0.38(12)	(1199.7)
5049.4	706.7(5)	0.45(12)	(1239.9)

Table 1. (continued)

E_1, keV	E_2, keV	$i_{\gamma\gamma}(\Delta i_{\gamma\gamma})$	$E_m(\Delta E_m)$, keV
5023.5	732.6(6)	0.40(13)	(1265.8)
4958.3	797.8(5)	0.43(12)	(1331.0)
4921.5	834.6(4)	0.98(19)	(1367.8)
4860.2	895.9(5)	0.58(16)	(1429.1)
4795.9	960.2(6)	0.48(16)	(1493.4)
4248.1	1508.0(5)	0.60(15)	(2041.2)
4142.7	1613.4(6)	0.45(15)	(2146.6)
4090.1	1666.0(6)	0.53(15)	(2199.2)
4051.9	1704.2(5)	0.54(15)	(2237.4)
4025.7	1730.4(4)	0.71(16)	(2263.6)
E_1+E_2 =5693.4 keV; E_f=591.8+595.8 keV			
5444.9	248.4(5)	0.86(24)	843.8(4)
5429.4	263.9(5)	0.78(23)	859.6(4)
5332.5	360.8(2)	1.36(20)	957.2(12)
5095.5	597.8(2)	1.67(23)	1193.7(7)
4979.8	713.5(1)	5.30(38)	1309.0(9)
4833.6	859.7(7)	0.80(28)	1456.6(11)
4772.0	921.3(4)	1.61(31)	1519.2(12)
4761.3	932.0(3)	1.59(27)	1528.0(3)
4607.1	1086.3(1)	2.83(30)	1681.7(7)
4576.7	1116.7(5)	0.78(23)	1712.7(5)
4539.4	1153.9(2)	2.00(26)	1749.8(4)
4512.4	1180.9(4)	1.06(24)	1776.9(4)
4457.7	1235.6(5)	0.85(24)	1831.5(4)
4030.6	1662.8(5)	0.93(25)	2258.8(8)
5384.7	308.7(4)	0.97(24)	(904.6)
5326.2	367.2(3)	1.22(20)	(963.1)
5300.7	392.7(2)	1.60(21)	(988.6)
5235.3	458.1(2)	1.79(22)	(1054.0)
5116.2	577.2(5)	0.85(23)	(1173.1)
5051.5	641.9(3)	1.16(23)	(1237.8)
4829.3	864.1(2)	2.18(33)	(1460.0)
4798.5	894.9(5)	0.94(27)	(1490.8)
4751.2	942.2(5)	0.97(27)	(1538.1)
4661.4	1032.0(4)	1.15(23)	(1627.9)
4555.0	1138.4(7)	0.72(25)	(1734.3)
4411.8	1281.6(5)	0.97(23)	(1877.5)
4407.9	1285.5(6)	0.83(23)	(1881.4)
3955.5	1737.9(5)	1.00(25)	(2333.8)
3929.0	1764.3(5)	0.92(25)	(2360.3)
3564.4	2129.0(5)	1.34(39)	(2724.9)

Notes to Table 1:

1. The E_m values in brackets were determined from relationship $E_m = B_n - E_1$ because analysis performed according to algorithm [3] did not allow determination of quanta ordering for these cascades.

2. The errors of determining E_1 and E_2 have the same magnitude but opposite signs in accordance with the algorithm [6] of numerical improvement of resolution.

3. At $E_2 < 520$ keV the $i_{\gamma\gamma}$ values are underestimated due to conditions of the experiment.

4. The intensities $i_{\gamma\gamma}$ for cascades with $E_1 + E_2 =$ 6289 and 5784 keV sum energies were normalized to a total area of doublet in the sum-coincidence spectrum. Normalizing coefficients to the total cascade intensities for these $i_{\gamma\gamma}$ are about 10 and about 1.5, respectively.

3. Spectroscopic information

Main conclusions about the properties of the ^{176}Lu nucleus are made in this article on the basis of the analysis of cascade γ-transitions summed over groups of their intermediate and final levels. But, the rather extensive information obtained in this experiment raises the point about its reliability and raises the question of its use. This is essentially because the decay scheme of ^{176}Lu obtained by us noticeably differs from that already published. So, we observed 81 secondary transitions populating levels below the excitation energy $E_m \approx 1.1$ MeV. Only 31 of them correspond to the data of Ref. 7 and only 23 to the data of Ref. 8. Such a serious discrepancy can be explained by the high probability of random coincidence of the γ-transition energies, what results in errors in the decay scheme designed using the Ritz combinatorial method. This effect can appear even for the data obtained with the crystal diffraction spectrometer. This statement can be easily checked if one builds, for example, the frequency distribution of sums $(E'_\gamma + E''_\gamma)$ in the vicinity of the difference of energies $(E'_f - E''_f)$ of any excited state. There are no serious grounds to relate the discrepancy between the data of Refs. 7 and 8, and those listed in Table 1 with any errors of the method used by us. The mean intensity of cascades, whose secondary transitions are placed in the decay scheme of Ref. 7 identically to Table 1, equals 0.046% and that of all 81 cascades equals 0.034% per decay.

It should be noted that the discrepancy between the decay schemes of ^{176}Lu obtained by us and by authors of Refs. 7 and 8 cannot be related only to the presence of γ-quanta following decay of the ^{177}Lu compound state. Such an effect would mean registration of random coincidences of the primary transitions in ^{176}Lu with γ-quanta in ^{177}Lu of quite a certain energy in the full energy peak in the sum-coincidence spectrum. Besides, the number of captures in ^{177}Lu is 5 times less than in the isotope under study. Also, there are no serious discrepancies in energies of levels established by us and in other articles.

However, the data of Table 1 unambiguously determine both the final level of a nucleus excited by a given cascade and the energy of cascade transitions. Therefore, the use of these data decreases to a great extent the role of random coincidences of the transition energies or differences between the level energies. Of course, the data in Table 1 are not completely free from false information. For example, the errors can be caused by the following effects:

(a) registration of a three-step cascade as a two-step one;

(b) registration of the first and third (fourth...) cascade transitions and random coincidence of their sum energy with the energy of any other two-step cascade within the limits of energy resolution of the spectrometer.

The influence of all kinds of sources of errors on the spectroscopic data were analysed in Ref. 4.

The absolute intensity of the three-step cascade observed as a pair of resolved peaks in the case (a) has been determined as:

$$i_{3\gamma} = 1/3 \times (p_3 \varepsilon_3) \times I_{\gamma\gamma}, \tag{1}$$

where p_3 is the probability of appearance of the third quantum after the decay of the level E'_g, ε_3 is the absolute efficiency of registration for the third-quantum and $I_{\gamma\gamma}$ is the total

absolute intensity of all two-step cascades populating level $E_g^{'}$. For the present experiment (certain detectors and isotope), the maximum of the effect under discussion should appear at the third quantum energy of a few hundred keV and must not exceed the value of about 10^{-4} per decay. This effect quickly decreases when increasing the excitation energy of the level depopulated by the third quantum. Such behaviour results from the decrease of the three values determining the effect. That is why this effect should be taken into account only in the analysis of the spectroscopic information at low excitation energy.

The second effect appears to be the strongest in nuclei with a high density of their low-lying levels (especially in odd-odd deformed nuclei). Corresponding data must be revealed and excluded from the results. Because the registration of the first ($E_1^{'}$) and the third (E_3) transitions does not differ from that of the first (E_1) and the second (E_2) transitions, this effect can be revealed only due to the exceeding the sums of the cascade absolute intensities $i_{\gamma\gamma}$ over the intensity i_1 of their primary transitions. This procedure was performed for the data in Table 1. It should be noted that the real contribution of the effect under consideration can appear only when the absolute value of the difference $|(E_1+E_2)-(E_1^{'}+E_3)|$ is considerably less than the width of peak in the sum-coincidence spectrum.

On the whole, the only way to obtain the most reliable decay scheme of deformed nucleus at the present level of the experiment is a complex analysis of the totality of available experimental data. It should be noted that the traditional methods of analysis of coincidences are not quite effective what is shown by the results of the use of "High Energy Resolution Array" for studying the decay scheme in ^{176}Lu [8].

Unlike the decay scheme, comparison between the energies of levels established in this work and in Refs. 7 and 8 demonstrates a better agreement. It should be noted that the E_m values in Table 1 were obtained independently from all previous experiments. When comparing, one should take into account that an insignificant number of the E_m values in Table 1, differing less than 1 – 2 keV, can correspond to the cascades proceeding via the same intermediate level. We kept this result in order to provide the best possible estimation of the level density [3] in the analysis described below. The data in Table 1 below 1 MeV contain information on two possible states of ^{176}Lu: 641 keV and 819 keV which are absent in the data published earlier. But if the potential level at 641 keV is excited by the only cascade with an intensity of about 0.8×10^{-4}, then level at 819 keV is populated by two cascades with a sum intensity of about 3.6×10^{-4} per decay. The former can be explained by unlikely random grouping of counts of the "noise" line or by the presence of a very intense (as compared with the other) cascade with the low-energy primary transition. In the second case, one cannot exclude the possibility that an unknown level of ^{176}Lu is observed in the experiment. Unfortunately, even analysis of the data on positions of peaks in sum-coincidence spectrum does not allow one to make more reliable conclusion about this point due to insufficient statistics and energy resolution.

We also observed the two-step cascades proceeding via three intermediate levels at 940, 963 and 972 keV, what contradicts the spin values assigned to these levels in Ref. 7. The rest are insignificant discrepancies between the data of Refs. 7 and 8 and Table 1 that can be explained, in principle, by conditions of previous experiments (insufficient energy resolution) and by possible combinations of systematic errors when studying cascade γ-decay. However, one cannot completely exclude the possibility of revealing unknown

levels, because any experiment has its own detection threshold. As compared with the previous (n,γ) measurements, the present experiment has the lowest detection threshold.

3.1. Contribution of ^{177}Lu

Not very large (as compared with the resolution of the spectrometer) spacing between the final levels in ^{176}Lu and the presence of weak full-energy peaks, and sufficiently strong single- and double-escape peaks related with the cascades in the ^{177}Lu isotope, cause the overlapping of a number of peaks in the sum-coincidence spectrum (see Fig. 1). This circumstance requires a proper correction of the spectroscopic information (Table 1) and the data on the sum intensities of cascades. This can be done in two ways:

(a) to correct (even though approximately) the corresponding data if the contribution of the background peak to the unresolved doublet in the sum-coincidence spectrum is insignificant (such a correction was performed for the data in Table 2

*TABLE 2. Total experimental intensities $I_{\gamma\gamma}$ (in % per decay) for two-step cascades with the fixed sum energy E_1+E_2 (*keV*). E_f is the energy (*keV*) of the final levels of cascades [7].*

E_1+E_2	E_f	$I_{\gamma\gamma}$
6289	0	[0.2][a]
6166	123	1.4(3)
6095	194	1.2(2)
6056	233+236	6.9(4)
5988	299+305	3.0(2)
5950	339	(0.3)
5917	372	2.7(5)
5903	381+386	2.8(3)
5852	433+437	4.7(6)
5839	450	1.8(2)
5825	464	3.2(5)
5802	488	1.1(1)
5784	505	[3.6][b]
5756	533	(4.5)
5693	596	(2.9)

Notes:
(a) the intensities of the doublet of the 6289 keV full-energy peak in ^{176}Lu and the single-escape peak (6803-511) keV in ^{177}Lu, are estimated from the ratio of approximated areas of these peaks;
(b) the intensity is estimated by subtraction of the extrapolated area of double-escape peak (6803-1022) keV in ^{177}Lu.

using the approximate values of the peak areas for corresponding doublets and singlets in the sum-coincidence spectrum);

(b) to reject cascades ending at a given final level of ^{176}Lu if the condition of relatively small contribution of background peak is not satisfied, or if areas of peaks of doublet cannot be estimated.

Situation (a) is observed for cascades to the ground state and to the final level at $E_f =$ 505 keV in ^{176}Lu. Condition (b) did not allow us to analyse cascades to the final level at 562 keV and the majority of final levels with $E_f > 600$ keV.

Experimental data on the most intense cascades in ^{177}Lu are already published [9]. This allowed us to identify and exclude background data from Table 2 using values for energies of low-energy quanta and ratios between the relative intensities of corresponding cascades in ^{177}Lu.

4. Analysis of experimental data

In order to reveal the main peculiarities of the γ-decay process, it is necessary to transform relative intensities of the observed cascades to the absolute values (in % per decay). This was performed by the normalization of relative intensities of the strongest cascades to their absolute values $I_{\gamma\gamma}$,

$$I_{\gamma\gamma} = I_\gamma \times br. \tag{2}$$

The absolute intensities I_γ of the corresponding primary transitions (5786, 5732, 5627, 5603, 5459, 5445, 5429, 5408, 5369, 5343, 5329, 5260, 5061, 5020, 4981, 4946, 4923, 4832 and 4771 keV) were taken from Ref. 10. The branching ratios *br* were determined from the standard spectra of coincidences with the same high-energy primary transitions which were constructed from the coincident events accumulated by us.

The results of this normalization are given in Table 2.

4.1. Dependence of the cascade intensities on energy of their intermediate levels

If the energies of intermediate cascade levels are not high (for example, less than 2 MeV for ^{176}Lu), then at least the main mass of the cascades appears as resolved peaks in the spectra like that shown in Fig. 2. According to Ref. 11, the portion of the intensity related to such cascades can be subtracted from the initial distribution and included in the dependence of the cascade intensity on the intermediate cascade-level energy (Fig. 3). If the sequence of quanta in these cascades (Table 1) is not determined by the algorithm of Ref. 3, then it can be set under the assumption that the transition with the higher energy is primary.

The continuous distribution remaining after subtraction of the areas of intense peaks is mainly formed by cascades with low-energy primary transitions and can also be included in the dependence mentioned above. However, for the cascades in ^{176}Lu whose intermediate level energies lie in the interval from 2 to ≈ 4 MeV, it is impossible to determine the quanta

ordering in this way and decompose their sum intensities into components corresponding to certain excitation energies. The dependence of cascade intensity on nuclear excitation energy at sufficiently high excitations is rather monotonous and the difference between the energies of primary and secondary transitions is not large. Therefore, (as suggested in Ref. 11), half of the intensity in this interval can be related to the primary transitions and the other half to secondary transitions. The main systematic uncertainty of this procedure in the total region of excitation energy is a redistribution of the cascade intensities between 0.5 MeV intervals of near the excitation energies E_f and $(B_n - E_f)$.

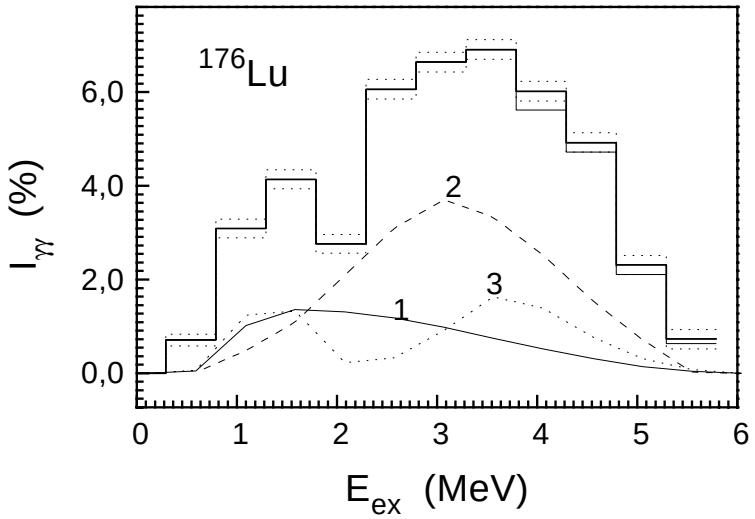

Fig. 3. Total two-step cascade intensities (in % per decay) as a function of the excitation energy. The histogram represents the experimental intensities summed in energy bins of 500 keV *with standard statistical errors; the largest possible estimates of probable systematic errors are shown by the additional solid histogram. Curves 1, 2 and 3 correspond to predictions according to models of Refs. 15, 16 and 18, respectively.*

This uncertainty also results from the fact that a portion of the low-intensity cascades with $E_m < 2$ MeV belongs to the "continuous" part of the intensity distributions (see Fig. 2). However, in the case of low energy of one of the cascade transitions, this uncertainty can be estimated. The method of estimation of the number of such unresolved cascades and their sum intensity was suggested in Ref. 12. That analysis is performed in the following way. Intensities of the cascades populating the same intermediate level E_m and different final levels E_f are summed. Such sum is a random value whose dispersion is mainly determined by the known fluctuation of the width of the cascade primary transition. For the sufficiently narrow interval of excitation energy E_m, the cumulative sum of the cascade intensities is approximated by the Porter-Thomas distribution. This allows the determination of the most probable number of excited states of a nucleus in the energy interval under consideration and the most probable value of sum intensity of cascades unresolved experimentally. Results of this analysis are given in Fig. 4 and the estimation of the systematic error obtained from this analysis is shown in Fig. 3.

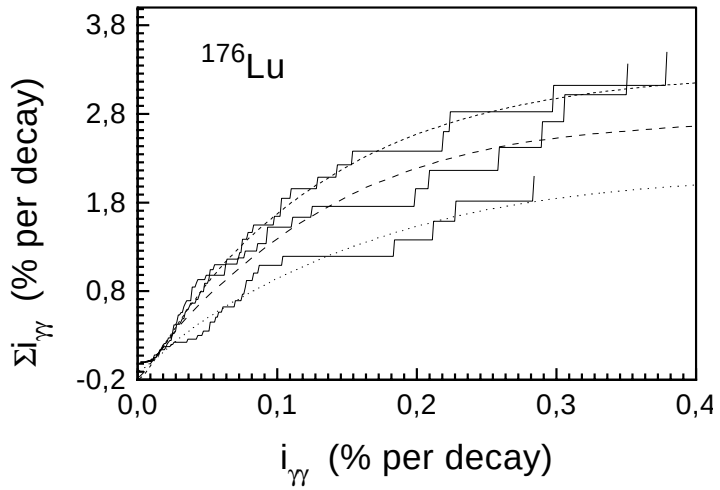

Fig. 4. Cumulative cascade intensities in ^{176}Lu *for three excitation-energy intervals:* $0.5-1.0$, $1.0-1.5$ *and* $1.5-2.0$ MeV *vs. the cascade intensity. Approximation and extrapolation of cumulative intensities to values corresponding to* $I_{\gamma\gamma}=0$ *is shown by the dashed lines.*

All experimental distributions (see Fig. 2) can be decomposed in this way. The sum of all "decomposed" spectra gives the dependence of the total two-step cascade intensity on the energy of the intermediate cascade levels.

Figure 3 presents the sums of the experimental cascade intensities (histograms with a $\Delta E = 500$ keV step) as a function of nuclear excitation energy. Cascade intensities $i_{\gamma\gamma}$ predicted by two models of radiative widths [13,14] and the level density model [15] are shown in this figure (curve 1) for comparison. The calculation was performed using the following relation:

$$i_{\gamma\gamma} = (\Gamma_{\lambda m}/\Gamma_{\lambda})(\Gamma_{mf}/\Gamma_{m}) < \rho_{m} > \Delta E. \tag{3}$$

Here $\Gamma_{\lambda m}$ and Γ_{mf} are the partial widths of transitions cascading through the levels $\lambda \to m \to f$, Γ_{λ} and Γ_{m} are the total widths of decaying states λ and m, respectively, and $< \rho_{m} >$ is the mean level density (for a given J^{π}) in the interval ΔE. Model intensities include cascades of $E1$, $M1$ and $E2$ transitions. The calculated cascade intensities shown in Fig. 3 are summed over all possible values of J^{π} of their intermediate levels m and over the corresponding final states f.

As in the case of the other deformed nuclei studied earlier, this comparison demonstrates the following characteristic properties:

(a) the experimental intensity exceeds the predictions of models that consider the nucleus as a system of non-interacting Fermi-particles;

(b) the discrepancy between the experimental and calculated results increases with increasing excitation energy;

(c) as for all nuclei studied earlier [2], the influence of the uncertainties of the model-

predicted partial widths on the cascade intensities is considerably less than influence of level density.

In order to reveal the factors causing this disagreement between experiment and calculation, a comparison with other models is necessary. This is done in Fig. 3, curves 2 and 3. In this modelling, two modifications of the notion of nuclear levels are made to account for the superfluid properties of the nucleus were used. The first of them [16,17] (curve 2) takes into account superfluidity of nuclear matter but only within the framework of the adiabatic approach — the energy of the phonon excitations is much less than that of the quasiparticle excitations. The second [9,18,19] uses the most general properties of thermodynamics of the second-order phase transition in order to account for the real situation, which contradicts the adiabatic approach at excitation energies of several MeV. In practice, the model of Refs. 18 and 19 uses known results from the experiments on thermodynamics of the transition from the superfluid to normal phases of a mixture of liquid ^{3}He and ^{4}He.

The densities of levels which are excited by the dipole transitions after the decay of the compound state with $J^\pi = 3^+, 4^+$, calculated within models Refs. 15, 16 and 18, are shown in Fig. 5 together with the number of levels observed by us below 2.4 MeV. For a comparison, at B_n, the calculated number is given of the excited states with $I = 2, 3, 4, 5$ of both parities (for the 100 keV excitation energy intervals). It was obtained for the average spacing [20] $D = 3.45(15)$ eV of $J^\pi = 3^+, 4^+$ neutron resonances. The number of the observed (Table 1) and shown in Fig. 5 low-lying levels is limited by the detection threshold, L_c, of individual cascade represented as a pair of peaks in the spectrum. The value of L_c depends on the statistics accumulated and on the number of background events. As can be seen in Fig. 4, L_c does not depend, in practice, on the excitation energy and is equal to about 10^{-4} events per decay. For this reason, only a part of excited states was observed in the experiment.

Comparison of the data in Figs. 3 and 5 allows one to make concrete conclusions about the adequacy of three models of level density for the experimental situation, and about the predictions given by the "best" model. As can be seen from the figures, the model suggested by Ignatyuk [16] and the model developed in Ref. 17 are suitable for predicting the level density above an excitation energy of 2 MeV. But this model does not correspond to reality at lower energies (it should be noted that these authors set B_n as the lower limit for the application of their model).

The model described in Refs. 9, 18 and 19 reproduces the density at excitation energies up to 3 MeV and, probably, overestimates it at higher energies of the nucleus under study (as may be seen in Fig. 3). It should be noted that the "minimum" in the level density predicted by this model is not an unremovable defect. For simplicity, the authors used the shape of the functional dependence of the specific heat of pure ^{4}He instead of a mixture of helium isotopes [21], which is more realistic, but requires more parameters.

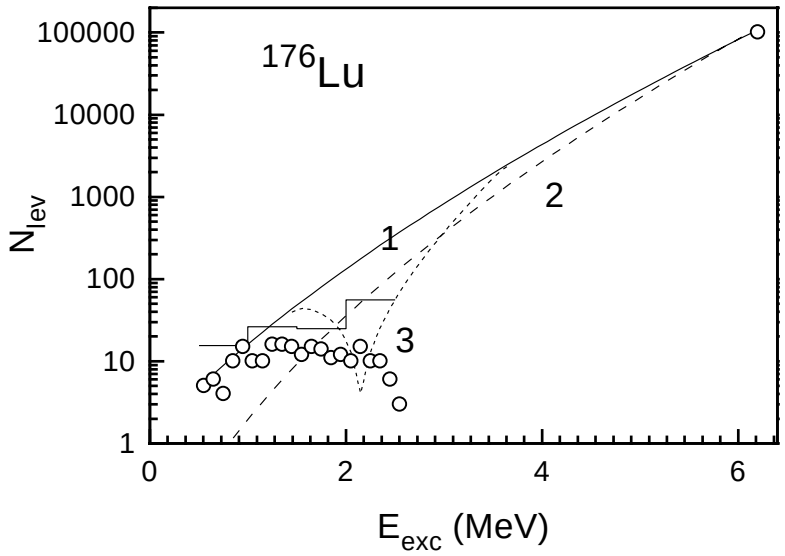

Fig. 5. The numbers of observed levels of the most intense cascades in ^{176}Lu *(Table 1) for an excitation energy interval of 100* keV*. Curves 1, 2 and 3 represent the predictions of models Refs. 15, 16 and 18, respectively. The histogram demonstrates the estimation of the level density from analysis of Ref. 12.*

In summary, one can conclude that a correct reproduction of the experimental situation in the cascade γ-decay of a deformed nucleus demands a more realistic model of level density excited in the (n,γ)-reaction than the Fermi-gas model. Such a model must unite the properties of models of Refs. 16, 17, 18 and 19, and to account, in a sufficiently realistic way, for the coexistence and interaction of fermion- and boson-type excitations at different energies of these systems. No conclusions about the application of such a model to other reactions can be made from an analysis of our results.

As was noted earlier [18], the data available on the properties of excited nuclear levels testify to a considerable influence of phonon-type excitations on the γ-decay process, whether the energy of these quanta of excitation is tens of keV (according to Ref. 17) or several hundred keV (according to Ref. 19). It would be worthwhile to test directly whether vibrational excitations exist and whether they somehow influence the probability of the cascade γ-decay of the compound state. In the situation where experimental determination of the structures of the observed states above 1 – 2 MeV is almost impossible, the only accessible way is the search for a possible regularity (harmonicity) in the spectra of the nuclear excitations. The first effort [19] at revealing the regularity proved that this effect is real.

A very simple and clear method of searching for the regularity in the spectra of the intermediate levels of the most intense cascades was suggested in Ref. 19. According to this method, the absolute intensities of individual cascades are smoothed in the vicinity of their intermediate level energies by a Gaussian curve with the parameter, for example, $\sigma = 25$ keV. The sum of these distributions over the total number of cascades included in

the analysis gives the spectrum $f(E)$ of the smoothed cascade intensities. The distorting influence of the global energy dependence of the cascade intensities can be reduced to considerable measure by the normalization

$$F(E) = f(E,\sigma)/f(E,\sigma = 250\ \text{keV}), \tag{4}$$

where the spectrum $f(E,\sigma = 250$ keV) is constructed from the same set of cascades. Analysis of the distributions $f(E)$ or $F(E)$, in order to search for groups of equidistant levels and to determine the equidistant period T, is performed by using the autocorrelation function

$$A(T) = \sum_E f(E) \times f(E+T) \times f(E+2T)\,, \tag{5}$$

and summation over the excitation energy E. The T value corresponding to the maximum of the functional $A(T)$ is taken as the equidistant period. The functional $A(T)$, however, can have several peaks. In order to make an unambiguous choice and to lower the probability that the T value is random, the following is suggested:

(a) the autocorrelation function be determined for the sets of cascade intensities differing in the registration threshold and in the parameter σ;

(b) this procedure be performed for all of the nuclei studied.

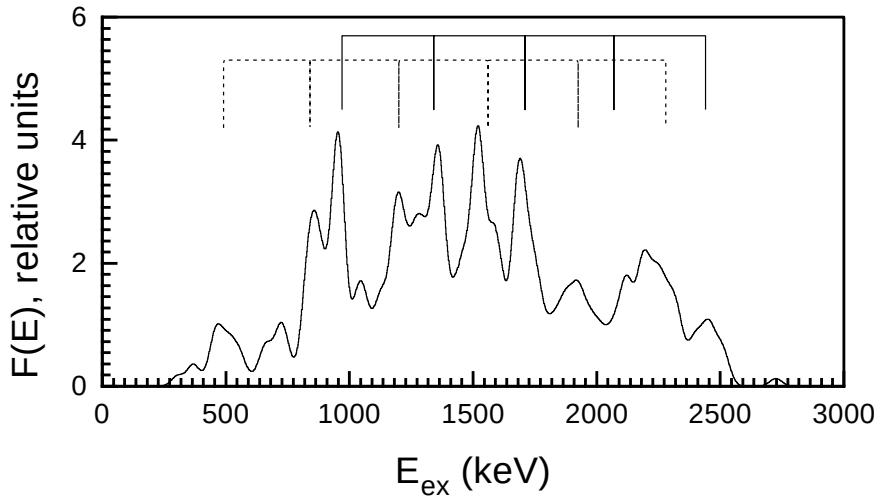

Fig. 6. The dependence of the cascade intensities (% per decay) listed in Table 1 on the excitation energy. Possible "bands" of harmonic excitations of the nucleus are marked; the Guassian-distribution parameter $\sigma = 25$ keV *was used.*

The relatively monotonous change of T at the transition to a neighbouring nucleus can be considered as an argument testifying to the considerable influence of nuclear harmonic vibrations on the excitation and decay probabilities of nuclear levels.

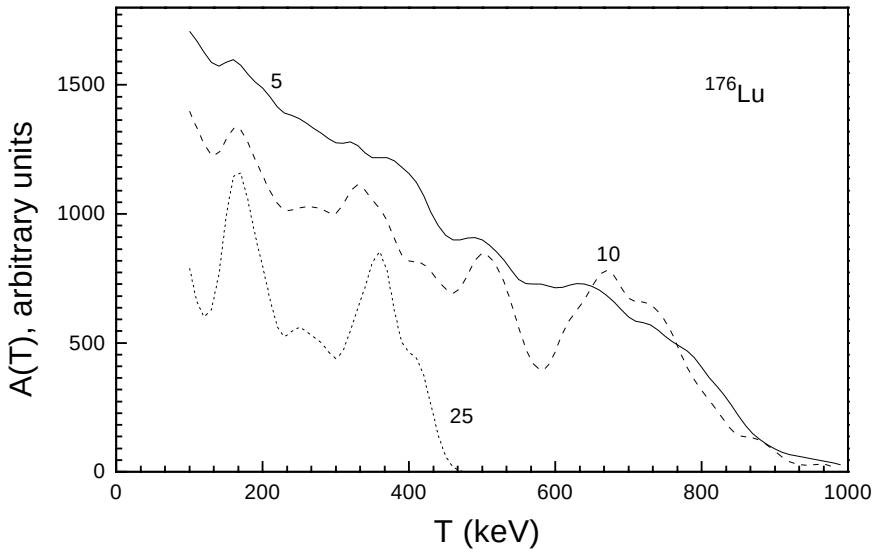

Fig. 7. The values of the functional $A(T)$ for different detection thresholds of the most intense cascades.

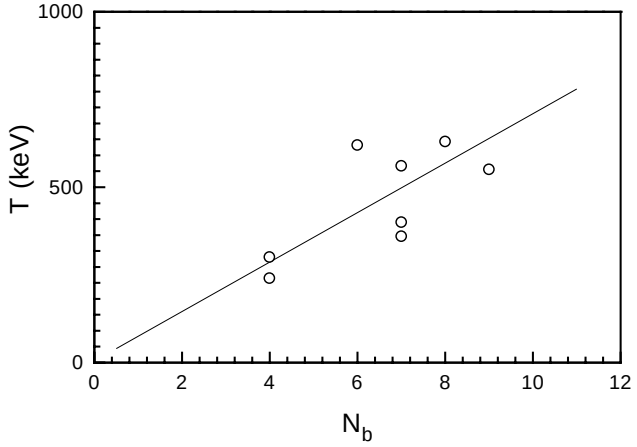

Fig. 8. The values of the equidistant period T for the odd-odd nuclei studied as a function of the number of boson pairs N_b in the unfilled shells. Line extrapolates the possible dependence.

Figure 6 shows the distribution $f(E)$ for ^{176}Lu, and Fig. 7 shows the corresponding autocorrelation functions. As can be seen in Fig. 7, the most probable equidistant period for this nucleus is about 360 keV. The probable vibrational "bands" (the groups of equidistant levels or their multiplets) are marked in Fig. 6. It was noted earlier [19] that the T values can be described by a linear function of the boson numbers, N_b, in the unfilled shells of nuclei. Figure 8 presents the value of the obtained equidistant period T for the following

odd-odd nuclei: ^{128}I, ^{160}Tb, ^{166}Ho, ^{170}Tm, ^{176}Lu, ^{182}Ta, ^{192}Ir and ^{198}Au. Here, the magic number $N = 100$ for the deformed potential [22] was taken into account when determining N_b. The observed dependence can be considered as an argument in favour of the possible existence of harmonic vibrations in nuclei, i.e., vibrational "bands" that are built on the high-lying ($E_{ex} > 1 - 2$ MeV) head states. The structures of the wave functions of these equidistant levels must differ by one or more phonons.

5. Conclusion

An experimental search for the cascade γ-decay process of the ^{176}Lu compound nucleus, following the thermal neutron capture in ^{175}Lu, has demonstrated the same peculiarities as those revealed for the nuclei studied earlier:

(a) the probable presence (dominance) of vibrational excitations below energies of 2 – 3 MeV which strongly influence on the cascade γ-decay;

(b) the clearly non-exponential dependence of the level density, which can be interpreted as the appearance of a transition from the mainly vibrational excitations (phonon energies of a few hundred keV) to excitations of quasiparticles.

Acknowledgements

Authors thanks are due to Ms. Ann Schaeffer for her help in preparation of the English version of this paper. This work was supported by GACR under the contract No. 202/96/0551 and by RFBR Grant No. 95-02-03848.

References

1) S. T. Boneva, E. V. Vasilieva, Yu. P. Popov, A. M. Sukhovoj and V. A. Khitrov, Sov. J. Part. Nucl. **22(2)** (1991) 232;

2) S. T. Boneva et al., Sov. J. Part. Nucl. **22(6)** (1991) 698;

3) Yu. P. Popov, A. M. Sukhovoj, V. A. Khitrov and Yu. S. Yazvitsky, Izv. AN SSSR, Ser. Fiz. **48** (1984) 1830;

4) S. T. Boneva, E. V. Vasilieva and A. M. Sukhovoj, Izv. AN SSSR, Ser. Fiz. **51** (1987) 2023;

5) J. Honzátko, K. Konečný, I. Tomandl, J. Vacík, F. Bečvář and P. Cejnar, Nucl. Instr. and Meth. **A376** (1996) 434;

6) A. M. Sukhovoj and V. A. Khitrov, Sov. J.: Prib. Tekhn. Eksp. **5** (1984) 27;

7) N. Klay, F. Käppler, H. Beer, G. Schatz, H. Börner, F. Hoyler, S. J. Robinson, K. Schreckenbach, B. Krusche, U. Mayerhofer, G. Hlawatsch, H. Linder, T. von Egidy, W. Andrejtscheff and P. Petkov, Phys. Rev. C **44** (1990) 2801;

8) K. T. Lesko, E. B. Norman, R.-M. Larimer, B. Sur and C. B. Beausang, Phys. Rev. C **44** (1990) 2850;

9) V. A. Khitrov, A. M. Sukhovoj, J. Honzátko, I. Tomandl and G. Georgiev, Fizika B **7** (1998) 37;

10) E. Browne, Nucl. Data Sheets **60** (1990) 227 A. Fubini, D. Prosperi, F. Terrasi and I. Vata, Nuovo Cimento A **8** (1972) 748;

11) S. T. Boneva, V. A. Khitrov, A. M. Sukhovoj and A. V. Vojnov, Z. Phys. A **338** (1991) 319; S. T. Boneva, V. A. Khitrov, A. M. Sukhovoj and A. V. Vojnov, Nucl. Phys. A **589** (1995) 293;

12) A. M. Sukhovoj and V. A. Khitrov, Yad. Fiz., **62** (N^o 1) (1999) to be published;

13) S. G. Kadmenskij, V. P. Markushev and W. I. Furman, Sov. J. Nucl Phys. **37** (1983) 165;

14) J. M. Blatt and V. F. Weisskopf, *Theoretical Nuclear Physics*, New York (1952);

15) W. Dilg, W. Schantl, H. Vonach and M. Uhl, Nucl. Phys. A **217** (1973) 269; T. von Egidy, H. H. Schmidt and A. N. Behkami, Nucl. Phys. A **481** (1988) 189;

16) A. V. Ignatyuk, *Proc. IAEA Consultants Meeting on the Use of Nuclear Theory*, in *Neutron Nuclear Data Evaluation*, Trieste, Italy (1975) IAEA-190, Vol.1, (1976) p. 211;

17) E. M. Rastopchin, M. I. Svirin and G. N. Smirenkin, Yad. Fiz. **52**, (1990) 1258 (in Russian);

18) S. T. Boneva, V. A. Khitrov, Yu. P. Popov and A. M. Sukhovoj, *In Capture Gamma-Ray Spectroscopy and Related Topics*, Budapest, Hungary, (October 1996), Vol. 1, p.483;

19) A. M. Sukhovoj and V. A. Khitrov, Izv. RAN, ser. fiz., **61** (1997) 2068;

20) S. F. Mughabghab, *Neutron Cross Sections*, V. 1, part B, Academic Press, New York (1984);

21) F. Gasparini and M. R. Moldover, Phys. Rev. Lett. **23** (1969) 749;

22) V. M. Strutinsky, A. G. Magner, S. R. Offengenden and T. Dossing, Z. Phys. A **346** (1993) 35.

GLAVNE POSEBNOSTI KASKADNOG RASPADA SLOŽENE JEZGRE ^{176}Lu

Primjenom sudesno-zbrojne metode, uz upotrebu dvaju Ge-detektora, proučavale su se dvostupne γ-kaskade nastale uhvatom termičkih neutrona u ^{175}Lu koje završavaju na 14 niskoležećih ($E_{uzb} < 600$ keV) stanja ili dubleta jezgre ^{176}Lu. Odredili su se parametri 350 najintenzivnijih kaskada. Veći njihov dio složen je u shemu raspada. Utvrdila se je pravilnost energija najintenzivnijih kaskada. Ishodi se uspoređuju s ranijim podacima za grupu sferičnih i izobličenih jezgri i s predviđanjima drugih modela.